Generalization of the one-dimensional ideal plasma flow with spherical waves

2006 J. Phys. A: Math. Gen. 39 7579

(http://iopscience.iop.org/0305-4470/39/23/027)

INSTITUTE OF PHYSICS PUBLISHING JOURNAL OF PHYSICS A: MATHEMATICAL AND GENERAL

J. Phys. A: Math. Gen. **39** (2006) 7579–7595 doi:10.1088/0305-4470/39/23/027

Generalization of the one-dimensional ideal plasma flow with spherical waves

Sergey V Golovin[1]

Queen's University, Kingston, Ontario K7 L 3N6, Canada

E-mail: sergey@mast.queensu.ca and sergey@hydro.nsc.ru

Received 9 February 2006, in final form 20 April 2006
Published 23 May 2006
Online at stacks.iop.org/JPhysA/39/7579

Abstract

We give a description of the ideal plasma flow, which is governed by an exact partially invariant solution of the magnetohydrodynamics equations. The solution generalizes known one-dimensional flow with spherical waves. The generalization consists in addition of the special tangent vector components of the velocity and the magnetic field at any plasma particle. In the special case of zeroth tangential component the solution coincides with the classical one-dimensional one. This paper describes a three-dimensional picture of the plasma flow, governed by the obtained solution.

PACS number: 52.30.Cv
Mathematics Subject Classification: 76W05, 76M60, 35C05

1. Introduction

This paper describes a partially invariant solution of the ideal magnetohydrodynamics equations. In some sense the solution under consideration generalizes the classical one-dimensional plasma flow with spherical waves. The classical solution determines a flow from a spherical source along the radius vector of each particle with a radial magnetic field. In the classical approach all functions are assumed to depend only on time and distance from the origin. In particular, this well-known solution could be used for modelling solar wind [1, 2]. Both, the classical one-dimensional solution and our generalized solution are generated by the group $O(3)$ of rotations admissible by the equations of ideal magnetohydrodynamics. The former solution is a singular invariant [3] with respect to $O(3)$ whereas the latter is a partially invariant one. We will demonstrate that the generalized solution describes a more complicated and interesting picture of this motion than the one-dimensional flow, which also exhibits some features of the classical solution.

[1] Permanent address: Lavrentyev Institute of Hydrodynamics, Novosibirsk 630090, Russia.

The construction of our generalized solution is based on the following assumptions.

- The spheres of constant radius $r = \text{const}$ are level surfaces of the solution, i.e. all invariant functions are constant on each level surface at fixed moment of time.
- The absolute values of normal and tangential vectors to the level surface components of the velocity and magnetic field are invariant functions. We also assume that the pressure and density of fluid are invariant functions. Thus, each quantity depends only on time t and distance r to the origin.
- The rotation angles of the velocity and magnetic field vectors about the normal to the level surface's vector are non-invariant functions. In other words they depend on all variables t, r, θ, φ (in the spherical frame of reference).

Thus, the generalization of the classical solution is achieved by permitting plasma motion and the magnetic field to spread in the direction tangential to spheres $r = \text{const}$. The investigation of the system of differential equations, which was obtained under these assumptions, was carried out in [14]. It was shown that the solution is non-trivial only when the velocity and magnetic field vectors have the same angle between their tangential to spheres $r = \text{const}$ components and meridians on the spheres. In other words, the radius vector of any particle is coplanar to its velocity and magnetic field vectors. The non-invariant function ω, which is the angle between the velocity and the meridional direction, changes from one particle on the level surface to another. The solution reduces to the classical one-dimensional one in the particular case when the tangential components of vectors vanish.

The investigation of the described solution is based on the examination of the over-determined system for function ω. It was proved that the solution reduces the original $(1 + 3)$-dimensional equations of ideal magnetohydrodynamics to an involutive system of partially differential equations with two independent variables t and r. Also, the solution involves a finite (non-differential) relation, which contains an arbitrary function and serves for the determination of the non-invariant function ω.

The analysis of the plasma motion, governed by the obtained solution, reveals the following characteristic properties:

- The trajectory of each particle as well as magnetic force lines that pass through the particle are flat curves belonging to the same plane. Each plane passes through the origin; its orientation is determined by traces of the vector fields on some level surface.
- The level surfaces $r = \text{const}$ are material, i.e. consist of the same particles for all moments of time.
- The solution is determined not in the whole three-dimensional space.

The latter property is a consequence of the well-known fact that the continuous tangent vector field on the sphere in odd-dimensional space does not exist. For proofs of the solution's properties and details we refer the reader to the paper [15].

The description of the plasma motion is performed in two steps. The first step is to solve the invariant system of partially differential equations with two independent variables with some initial data. Its solutions define the shape of the trajectories and magnetic force lines as well as dependence of the thermodynamical functions on time t and radial coordinate r. The second step is substituting invariant functions into the implicit finite equation for the function ω. Its solution defines $\omega(t, r, \theta, \varphi)$ providing the position and orientation of the trajectories and magnetic field lines in the three-dimensional space. This gives a complete picture of plasma motion, governed by this solution.

At first, the solution of the observed type was constructed for the ideal gas dynamics in [4]. Investigation of the particular classes of solutions (self-similar, stationary, projective-invariant) to the gas dynamics equations was carried out in [5, 6]. In all these works it was

shown that the solution is defined only outside of the sphere $r = r_*$, where the boundary is observed as a source or drain of fluid. In the stationary solution the boundary is unmovable, and in the non-stationary solutions the boundary r_* moves as time grows.

The generalized one-dimensional solution with spherical waves is usually referred to as 'the singular vortex'. This name was first used in [4] for the solution of this type with the initial data, continuous on the sphere $r = r_0$ without poles. Later on this name became applicable to all class of observed solutions. Another name in use is 'Ovsiannikov's vortex' according to the name of the author of the pioneering work [4].

The partially invariant solution with respect to the group $O(3)$ of rotations to the equations of incompressible and compressible ideal fluid was also observed in [7, 8]. It is known that the analogous solution for the Navier–Stokes equations is reducible to the classical one-dimensional one [9].

In this work a geometrical interpretation of the solutions of the implicit equation for the non-invariant function ω is proposed. This equation contains an arbitrary function of one argument. It is shown that this function defines some curve γ on each sphere $r = \text{const}$. At each section $r = r_0$ the solution $\omega = \omega(t, r_0, \theta, \varphi)$ is determined only inside the stripe on the sphere, bounded by equidistants to the curve γ. The width of the stripe is determined from the solution of the invariant subsystem and depends on t and r. The boundary of the stripe could have a singularity of the 'dovetail' type. In this case it is impossible to determine a solution, continuous over the dovetail. The criterion of the absence of singularities of the boundaries of the stripe in terms of geodesic curvature of γ is found.

The geometrical interpretation allows the construction of a picture of plasma motion as a whole. It is demonstrated by an example of stationary plasma flow with a constant density. In the stationary solution the magnetic field is collinear to the velocity; therefore, the streamlines coincide with the magnetic force lines. The flow in the example is generated by a spherical source of plasma. Each particle moves over the same flat trajectory; however, the orientation of each plane depends on the initial position of the particle. The flow tends to the radial one at the infinite distance from the source. All particles approach the surface formed by the ray, which origins at the source and slides along the curve γ on the sphere.

2. Preliminary information

The non-stationary motion of an infinitely conducting plasma is described by the following system of equations:

$$\begin{aligned} &D\rho + \rho \operatorname{div} \mathbf{u} = 0, \\ &D\,\mathbf{u} + \rho^{-1}\nabla p + \rho^{-1}\mathbf{H} \times \operatorname{rot} \mathbf{H} = 0, \\ &Dp + A(p, \rho) \operatorname{div} \mathbf{u} = 0, \\ &D\,\mathbf{H} + \mathbf{H} \operatorname{div} \mathbf{u} - (\mathbf{H} \cdot \nabla)\,\mathbf{u} = 0, \\ &\operatorname{div} \mathbf{H} = 0,\ D = \partial_t + \mathbf{u} \cdot \nabla. \end{aligned} \tag{2.1}$$

Here $\mathbf{u}$ is the velocity vector, p is the pressure, ρ is the density and $\mathbf{H}$ is the magnetic field vector. All functions depend on time t and coordinates $\mathbf{x} = (x, y, z)$. The function $A(p, \rho) = \rho c^2$ ($c = \sqrt{\partial p/\partial \rho}$ is a thermodynamical speed of sound) is determined by the plasma state equation $p = f(\rho, S)$, where S denotes the entropy. For example, the state equation of the polytropic gas is $p = S\rho^{\kappa}$ where κ is a polytropic exponent. The corresponding function A is $A(p, \rho) = \kappa p$. For known velocity and magnetic vector fields one can find the electric field $\mathbf{E}$ and the electric current density $\mathbf{j}$ by $\mathbf{E} = -\mathbf{u} \times \mathbf{H}$ and $\mathbf{j} = \operatorname{rot} \mathbf{H}$.

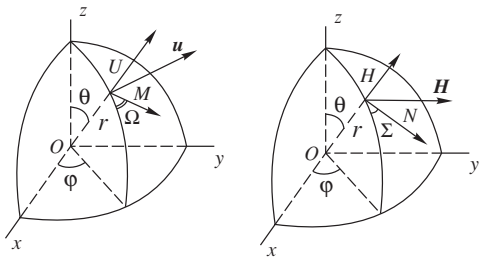

Figure 1. The decomposition of the velocity vector **u** and magnetic field vector **H** according to the spherical frame of reference. The vectors are characterized by their normal and tangential to spheres $r = \text{const}$ components and by angles between the tangential components and the meridional direction.

The complete group of transformations admitted by system (2.1) was calculated in [10] (see also [11]). It has a subgroup $O(3)$ of simultaneous rotations in the spaces $\mathbb{R}^3(\mathbf{x})$, $\mathbb{R}^3(\mathbf{u})$ and $\mathbb{R}^3(\mathbf{H})$. The classical one-dimensional solution with spherical waves, which is symmetric with respect to the group $O(3)$, has a representation

$$\mathbf{u} = U(t,r)\mathbf{x}, \qquad \mathbf{H} = H(t,r)\mathbf{x}, \qquad \rho = \rho(t,r), \qquad p = p(t,r). \tag{2.2}$$

Here $\mathbf{x}$ is a radius vector of a plasma particle, and $r = \sqrt{x^2+y^2+z^2}$. Functions U, H, ρ and p are determined from the involutive system of differential equations with two independent variables. From the group-theoretical point of view [3] solution (2.2) is a singular invariant solution with respect to the group $O(3)$. Another interpretation of solution (2.2) in terms of weak transversality is given in papers [12, 13]. However, the admissible group $O(3)$ allows the construction of another type of solution, namely, a partially invariant one.

In the space of independent variables $\mathbb{R}^3(x,y,z)$ we introduce a spherical frame of reference (r,θ,φ) according to

$$x = r\sin\theta\cos\varphi, \qquad y = r\sin\theta\sin\varphi, \qquad z = r\cos\theta. \tag{2.3}$$

An arbitrary vector $\mathbf{a} = (u,v,w)$ has the following decomposition in the above spherical frame:

$$\begin{aligned} u_r &= u\sin\theta\cos\varphi + v\sin\theta\sin\varphi + w\cos\theta,\\ u_\theta &= u\cos\theta\cos\varphi + v\cos\theta\sin\varphi - w\sin\theta,\\ u_\varphi &= -u\sin\varphi + v\cos\varphi. \end{aligned} \tag{2.4}$$

To denote the components of velocity and magnetic field vectors we use the following individual notation:

$$\begin{aligned} &v_r = U, \qquad v_\theta = M\cos\Omega, \qquad v_\varphi = M\sin\Omega;\\ &H_r = H, \qquad H_\theta = N\cos\Sigma, \qquad H_\varphi = N\sin\Sigma. \end{aligned} \tag{2.5}$$

Here U and H are radial components of vectors **u** and **H** correspondingly. Functions M and N determine the tangential to spheres $r = \text{const}$ components of the vectors. Notation Ω and Σ are used for the angles between the vectors **u**, **H** and the meridional direction on the sphere (see figure 1). In these notation the invariants of the group $O(3)$ can be written as

$$t, \quad r, \quad U, \quad M, \quad H, \quad N, \quad \Omega - \Sigma, \quad p, \quad \rho. \tag{2.6}$$

According to the algorithm [3] the representation of the partially invariant solution has the following form:

$$\begin{aligned} &U = U(t,r), \qquad M = M(t,r), \qquad H = H(t,r), \qquad N = N(t,r),\\ &\Sigma = \phi(t,r) + \omega(t,r,\theta,\varphi), \qquad \Omega = \omega(t,r,\theta,\varphi), \qquad p = p(t,r),\ \rho = \rho(t,r). \end{aligned} \tag{2.7}$$

Representation (2.7) involves the invariant functions U, M, H, N, ρ and p, which depend only on the variables t and r, and a non-invariant function ω, which depends on all independent variables. In the case $M = N = 0$ solution (2.7) coincides with the classical solution (2.2). In comparison with the classical one-dimensional solution, representation (2.7) has a non-zero tangential to the spheres $r = \text{const}$ components of the vectors $\mathbf{u}$ and $\mathbf{H}$. The thermodynamical functions, as well as in the classical solution, depend only on t and r.

Substitution of representation (2.7) into (2.1) gives a system of equations for the invariant functions and an overdetermined system for the non-invariant function ω. The latter system is to be observed on the solutions of the former. Investigation of compatibility of these systems was carried out in [14]. At that only the irreducible solutions were taken into account, i.e. solutions where function ω is determined with functional arbitrariness. In order to describe the resulting system of the equations it is convenient to introduce the following notations:

$$M_1 = \frac{M}{r}, \qquad H = \frac{H_0}{r^2 \cos\tau}, \qquad N_1 = rN. \tag{2.8}$$

Here H_0 is an arbitrary constant, and $\tau \in (-\pi/2, \pi/2)$ is some function of t and r. The following statement was proved in [14].

Theorem 1. *The solution to the ideal magnetohydrodynamics equations (2.1) of the form (2.7) with functional arbitrariness in the determination of the function ω exists only when $\phi \equiv 0$. At that the velocity and the magnetic field vectors at any particle are coplanar to its radius vector. The invariant functions are determined from the invariant system of equation*

$$\begin{aligned}
&D_0 M_1 + \frac{2}{r} U M_1 - \frac{H_0}{r^4 \rho \cos\tau} N_{1r} = 0,\\
&D_0 N_1 + N_1 U_r - \frac{H_0}{\cos\tau} M_{1r} - M_1 N_1 \tan\tau = 0,\\
&D_0 p + A(p,\rho)\left(U_r + \frac{2}{r}U - M_1 \tan\tau\right) = 0,\\
&D_0 U + \frac{1}{\rho} p_r + \frac{N_1 N_{1r}}{r^2 \rho} - r M_1^2 = 0, \qquad H_0 \tau_r = N_1 \cos\tau,\\
&D_0 \rho + \rho\left(U_r + \frac{2}{r}U - M_1 \tan\tau\right) = 0, \qquad D_0 \tau = M_1,\\
&D_0 = \partial_t + U\partial_r.
\end{aligned} \tag{2.9}$$

The non-invariant function ω is defined by the following implicit equation:

$$F(\eta, \zeta) = 0. \tag{2.10}$$

Here F is an arbitrary smooth function of the following arguments:

$$\begin{aligned}
&\eta = \cos\theta \sin\tau - \sin\theta \cos\omega \cos\tau,\\
&\zeta = \varphi + \arctan \frac{\sin\omega \cos\tau}{\cos\theta \cos\omega \cos\tau + \sin\theta \sin\tau}.
\end{aligned} \tag{2.11}$$

3. The stationary solution

In [15] particular solutions of system (2.9) were constructed and investigated. The symmetry group of system (2.9) was calculated. It was shown that there exist four sufficiently different invariant solutions, which reduce system (2.9) to a system of ordinary differential equations. Namely, these are stationary, self-similar, homogeneous and logarithmic solutions. The

corresponding system of equations was analysed. In this work we restrict ourselves to the case of the stationary solution. However, the general properties of plasma motion are similar to the other subclasses of solutions.

It was shown that in the stationary solution the vectors **u** and **H** are collinear, i.e. the streamlines coincide with the magnetic force lines. The description of the solution is easily performed with the aid of generalized potential σ introduced by the formula

$$\tau = 2\arctan\left[\tanh\left(\frac{1}{2}\sigma\right)\right]. \tag{3.1}$$

In terms of σ the expressions for the sought functions have the following form:

$$M_1 = \frac{1+H_0^2\sigma'}{r^2}, \qquad N_1 = H_0\sigma', \qquad \rho = \frac{\sigma'}{1+H_0^2\sigma'}, \qquad U = \frac{(1+H_0^2\sigma')}{\sigma'}\frac{\cosh\sigma}{r^2}. \tag{3.2}$$

We may determine σ from the implicit equation

$$\left(\frac{1+H_0^2\sigma'}{\sigma'}\right)^2\frac{\cosh^2\sigma}{r^4} + \frac{2\kappa S_0}{\kappa-1}\left(\frac{\sigma'}{1+H_0^2\sigma'}\right)^{\kappa-1} + \frac{\left(1+H_0^2\sigma'\right)^2}{r^2} = b^2. \tag{3.3}$$

Here κ is an adiabatic exponent of fluid. Representation (3.2) does not work for incompressible plasma flows. In the case of constant density it is convenient to use the following representations in terms of an invariant function τ:

$$M_1 = \frac{H_0^2\tau'}{r^2\cos\tau}, \qquad N_1 = \frac{H_0\tau'}{\cos\tau}, \qquad U = \frac{H_0^2}{r^2\cos\tau}, \qquad \rho = \frac{1}{H_0^2}. \tag{3.4}$$

For a flow with a constant pressure the function $\tau(r)$ must satisfy the following equation:

$$\tau'^2 = r^2\cos^2\tau - r^{-2}. \tag{3.5}$$

Note that solutions (3.4) and (3.5) belong to the class of incompressible stationary plasma motions investigated in the paper [16]. The infinite-dimensional pseudogroup of transformations obtained in this work could be used to generalize solutions (3.4) and (3.5).

The further description of the generalized one-dimensional plasma flow with spherical waves will be given on an example of particular solutions (3.4) and (3.5). This case allows us to demonstrate the geometric features of the plasma flow in the three-dimensional space without the necessity to go into the details of investigation of the invariant system (2.9).

Let us outline the main properties of solutions (3.4) and (3.5) as proved in [15]. The solution is determined in the stripe $-\pi/2 < \tau < \pi/2$ provided that $r^2\cos\tau \geqslant 1$. The curve $r^2\cos\tau = 1$ is a limit line for solution (3.4), which means that the solution cannot be extended behind this curve.

Equation (3.5) has two symmetrical families of the solutions: increasing and decreasing ones. They correspond to two different choices of the sign of the derivative τ' after taking the square root of both sides of equation (3.5). According to definition (2.5) the tangent components M_1 and N_1 have to be positive. This is only possible for increasing solutions $\tau(r)$ of equation (3.5). The picture of typical increasing integral curves of this equation is shown in figure 2. The horizontal lines show the asymptotes $\tau = \pm\pi/2$. It was proved that the integral curves asymptotically approach the limit curve $r^2\cos\tau = 1$ whenever $r \to \infty$ (the limit curve is a dashed curve in figure 2). This means that at a large distance from the origin

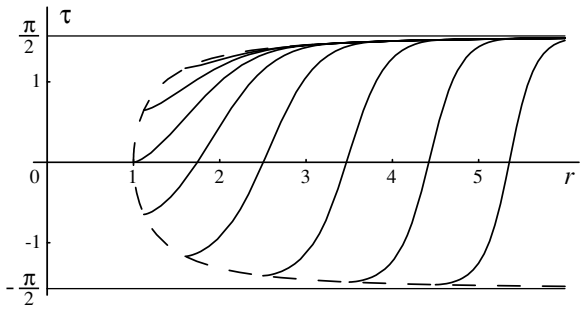

Figure 2. The typical set of increasing integral curves of equation (3.5). The dashed curve is a limit line $r^2 \cos\tau = 1$.

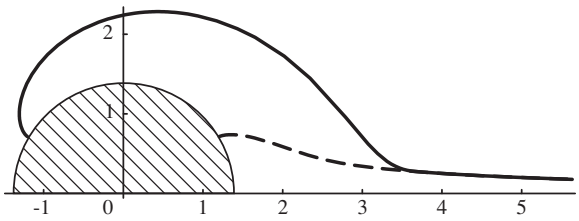

Figure 3. Typical magnetic field lines in the stationary solutions (3.4) and (3.5). The initial data are $\tau(r_0) = \pm\arccos(1/r_0^2)$ with $r_0 = 1.4$. The solid curve corresponds to the negative sign of $\tau(r_0)$. The curves will be referred to as 'long' and 'short' magnetic curves. At $r \to \infty$ both long and short magnetic field curves approach the ray $\tau = \pi/2$.

the velocity and the magnetic vector fields are close to the radial ones:

$$U \sim H_0^2, \qquad M \sim \frac{2H_0^2}{r^2}, \qquad H \sim H_0, \qquad N \sim \frac{2H_0}{r^2}.$$

The condition of non-negativity on the right-hand side of equation (3.5) gives a restriction on the domain of the solution. It follows from figure 2 that the solution cannot be extended up to the origin $r = 0$. Hence, the solution is determined only outside some spherical source or drain of the plasma. The radius of this source is defined by the minimal value of the independent variable r along the chosen integral curve of equation (3.5).

The typical magnetic field lines (or streamlines) in the stationary solution for the incompressible plasma are shown in figure 3. The two magnetic lines, which are determined by two different integral curves of equation (3.5), are shown. Both integral curves originate on the limit circle $r = 1.4$ with symmetrical initial data $\tau(1.4) = \pm\arccos(1/1.96) \approx \pm 1.04$. The solid curve corresponds to the negative initial value of τ. Asymptotic behaviour at $r \to \infty$ is the same for all magnetic lines.

The choice of an integral curve of equation (3.5) (or (3.3)) defines all the sought functions according to formula (3.4) (or (3.2)). All magnetic force lines, which begin on the same sphere, have the same shape. However, the orientation of the magnetic field lines in the three-dimensional space is determined by the direction of the magnetic vector field on some initial sphere. This directional field is determined by the solution of the implicit equation (2.10) for the function ω. Thus, the complete picture of the plasma motion is non-trivial. In the following sections we give a geometrical interpretation of the solution of an implicit equation (2.10) and an algorithm to describe the plasma motion as a whole.

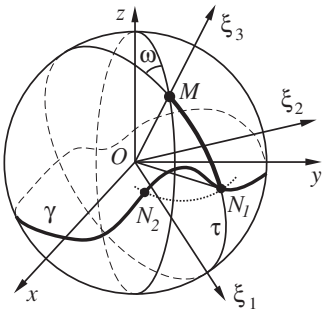

Figure 4. The definition of the $O\xi_1\xi_2\xi_3$ Cartesian frame of reference.

4. The initial vector field on the sphere

In order to give a geometrical interpretation of the solution $\omega = \omega(t, r, \theta, \varphi)$ for the implicit equation (2.10), the following auxiliary construction is introduced. Let us observe an arbitrary point M on the unit sphere, defined by angles (θ, φ) in the spherical frame of reference (2.3).

Suppose that function ω is defined at M. Let us introduce an auxiliary Cartesian frame of reference $O\xi_1\xi_2\xi_3$, which relates to M in the following way. The axis $O\xi_3$ passes through the origin O and point M. The axis $O\xi_1$ is orthogonal to the axis $O\xi_3$ in the origin O and belongs to the plane, which is determined by the angle $\omega(M)$ as shown in figure 4. The axis $O\xi_2$ is orthogonal to $O\xi_1$ and $O\xi_3$ such that the frame $O\xi_1\xi_2\xi_3$ has a positive orientation.

A transformation from the frame $Oxyz$ to the frame $O\xi_1\xi_2\xi_3$ can be performed by the subsequent action of the following rotations:

- about the Oz-axis on the angle φ (precession);
- about the $O\xi_2$-axis on the angle θ (nutation) and
- about the $O\xi_3$-axis on the angle ω (proper rotation).

The coordinates of any point on a sphere could be expressed in both $Oxyz$ and $O\xi_1\xi_2\xi_3$ frames of reference. Let us denote the coordinate triple in the frame $Oxyz$ as $\mathbf{r}$; the coordinate triple in the frame $O\xi_1\xi_2\xi_3$ as $\mathbf{R}$. The relation between triples $\mathbf{r}$ and $\mathbf{R}$ is given by

$$\begin{aligned} \mathbf{R} &= \Gamma_{12}(\omega)\Gamma_{13}(\theta)\Gamma_{12}(\varphi)\mathbf{r}, \\ \mathbf{r} &= \Gamma_{12}(-\varphi)\Gamma_{13}(-\theta)\Gamma_{12}(-\omega)\mathbf{R}, \end{aligned} \tag{4.1}$$

where $|\mathbf{r}| = |\mathbf{R}| = 1$ and Γ_{ij} are the orthogonal operators

$$\Gamma_{12}(\alpha) = \begin{pmatrix} \cos\alpha & \sin\alpha & 0 \\ -\sin\alpha & \cos\alpha & 0 \\ 0 & 0 & 1 \end{pmatrix}, \qquad \Gamma_{13}(\alpha) = \begin{pmatrix} \cos\alpha & 0 & -\sin\alpha \\ 0 & 1 & 0 \\ \sin\alpha & 0 & \cos\alpha \end{pmatrix}. \tag{4.2}$$

Note that the coordinate plane $O\xi_3\xi_1$ contains both trajectory and magnetic field lines passing through the point M at the initial time moment $t = t_0$. In the reference frame $O\xi_1\xi_2\xi_3$ point M has coordinates $(0, 0, 1)$. The motion of the plasma particle, located at M at $t = t_0$, could be described by its polar coordinates $(r\sin\psi, 0, r\cos\psi)$ at $t > t_0$. Here r and ψ are polar coordinates of the particle in the plane $O\xi_3\xi_1$.

Let us observe vector $\mathbf{R}_\tau = (\cos\tau, 0, \sin\tau)$. According to formula (4.1) it has the following coordinates in the $Oxyz$ frame of reference:

$$\mathbf{r}_\tau = (a, b, \eta). \tag{4.3}$$

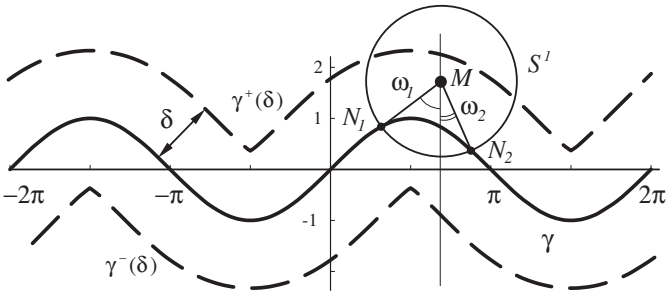

Figure 5. The planar analogue of the construction of theorem 2. For the chosen curve γ there are two possible solutions ω_1 and ω_2 at any point inside the stripe between the equidistants $\gamma^{\pm}(\delta)$.

Here η is determined by formula (2.11). The values of a and b are

$$\begin{aligned} a &= \cos\theta\cos\tau\cos\varphi\cos\omega + \cos\varphi\sin\theta\sin\tau - \cos\tau\sin\varphi\sin\omega, \\ b &= \cos\theta\cos\tau\sin\varphi\cos\omega + \sin\varphi\sin\theta\sin\tau + \cos\tau\cos\varphi\sin\omega. \end{aligned} \tag{4.4}$$

With the value ζ from (2.11) the following equalities are correct:

$$\cos\zeta = \frac{a}{\sqrt{a^2+b^2}}, \qquad \sin\zeta = \frac{b}{\sqrt{a^2+b^2}}. \tag{4.5}$$

The key point of our observation is the following interpretation of relations (4.3)–(4.5). We conclude, that the point $\mathbf{r}_\tau$ belongs to the unit sphere. It raises above the Oxy plane on the height η. The projection of the point $\mathbf{r}_\tau$ onto the Oxy plane deviates from the Ox axis on the angle ζ. The obtained values η and ζ are related by equation (2.10).

We shall look at the same result from another point of view. Let relation (2.10) determine a curve γ on the unit sphere S^2. The value η is a height of γ above the plane Oxy and the value ζ is a deviation angle of the projection of the point onto the Oxy plane from the positive direction of the Ox axis (see figure 4). For a given point M, which is defined by its spherical coordinates (θ, φ), let us draw a circle S^1 on the sphere S^2 with the centre M and geodesic radius $\pi/2 - \tau$ (the value τ is the same for all points of S^2). Let N_i, $i = 1, \ldots, k$ be the points of intersection of the curve γ with the circle S^1. From the above construction it follows that the angles between the meridian, which passes through M, and the geodesic curves, which follow from M to each N_is, define all possible values of the angle ω, which satisfy relation (2.10).

Theorem 2. *Let M be a point on the unit sphere S^2 and $S^1 \subset S^2$ is a circle on the sphere S^2 with the centre M and the geodesic radius $\pi/2 - \tau$. Let relation (2.10) determine the curve $\gamma \subset S^2$ and N_i, $i = 1, \ldots, k$ are the points of intersection of S^1 and γ. For each $i = 1, \ldots, k$ the angle between the meridian in the point M and the geodesic of length $\pi/2 - \tau$, which passes from M to N_i, determines the solution of the implicit equation (2.10) for function $\omega(\tau, \theta, \varphi)$. All solutions of equation (2.10) could be determined in this way.*

5. Planar analogue

Let us illustrate the statement of theorem 2 in a planar case. A similar construction is represented in figure 5. An analogue of the sphere S^2 is a plane; we have chosen the curve γ to be a sinusoid. The circle with a centre at point M and radius $\pi/2 - \tau$ has two points N_1 and

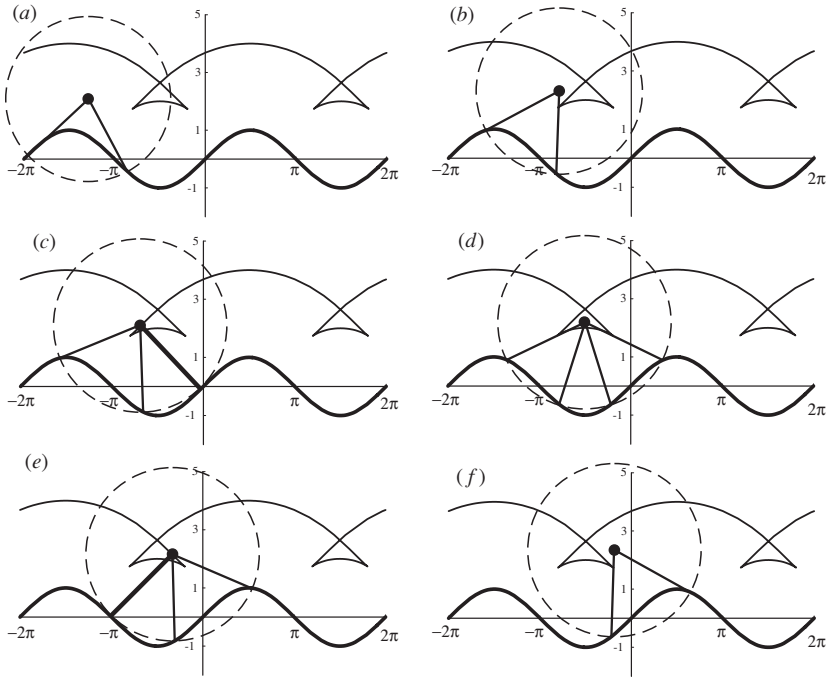

Figure 6. The behaviour of the branches of function ω over the dovetail. There are two branches of ω outside the dovetail in figures (*a*), (*b*) and (*f*); three branches of ω at the borders of the dovetail in figures (*c*) and (*e*); and four branches of solution inside the dovetail in figure (*d*).

N_2 of intersection with the curve γ. Angles between the line segments MN_i and the vertical line (analogue of the meridian) give two possible values for ω. Let us denote as $\gamma^{\pm}(\delta)$ the equidistant curves for γ, which are shifted on the geodesic distance δ from the curve γ. The sign '+' corresponds to the shift of equidistant to the north; the sign '−' denotes the shift to the south.

The main features of the dependence of $\omega(\tau, \theta, \varphi)$ defined by theorem 2 are as follows:

- The dependence $\omega(\tau, \theta, \varphi)$ is multiple valued. There is an even number of branches of the function ω as the circle S^1 is not tangent to γ at any point. The odd number of branches is possible only when there is an odd number of tangency points of S^1 and γ.
- The function ω is determined only in the stripe of the geodesic width $\pi - 2\tau$ with the medial line γ. In the points of equidistants $\gamma^{\pm}(\pi/2 - \tau)$ the segment MN is directed orthogonal to the equidistants towards the curve γ.
- There could be singularities of the dovetail type on the equidistants $\gamma^{\pm}(\delta)$. It is impossible to choose a branch of function $\omega(\tau, \theta, \varphi)$, which remains continuous when point M moves across all boundaries of the dovetail. Any branch of function ω is discontinuous over some boundary of the dovetail.

The latter statement is illustrated in figure 6. Here the curve γ is a sinusoid, the same as in figure 5. The shift δ of the equidistants $\gamma^{\pm}(\delta)$ is large enough to evoke the dovetail overlaps of the equidistants. Let us choose a point inside the stripe between the sinusoid and equidistant as in figure 6(*a*). There are two branches of the solution at this point. Let us move the point towards the dovetail, figure 6(*b*). When the point reaches the left boundary of the dovetail the

new branch of solution appears as depicted in figure 6(*c*). In the subsequent motion of the point inside the dovetail the new branch of solution splits into two branches, in other words there are four branches of the solution inside the dovetail, figure 6(*d*). On the right-hand side of the dovetail two 'old' branches of the solution stick together, figure 6(*e*), and disappear when the point comes out of the dovetail, figure 6(*f*).

Hence, if the point moves from the left to the right, then the line of discontinuity of the function ω is the right-hand side of the dovetail. Conversely, if the point moves from the right to the left, then the line of discontinuity is the left-hand side of the dovetail. In any case, there should be a line of discontinuity inside the dovetail, which 'switches' the branches of solution from the left-hand side of the dovetail to the branches from the right-hand side.

The only way to prevent the discontinuity is to observe the stripe, which does not have dovetails on its boundaries. In the next paragraph we determine the width of the stripe, which guarantees the absence of the dovetails.

6. Criterion of the non-singularity of the initial vector field

Let us find the maximal distance δ, such that the equidistants $\gamma^{\pm}(\delta)$ do not have dovetail singularities. We begin with the planar case.

Theorem 3. *Let γ be a smooth planar curve. The equidistants $\gamma^{\pm}(\delta)$ are smooth curves as well if and only if the following inequality holds:*

$$\delta < \min_{\mathbf{x}\in\gamma} R(\mathbf{x}). \tag{6.1}$$

Here R is the radius of curvature of the curve γ.

Proof. Let us introduce a natural parameter s along the curve γ. Let $\mathbf{n}$ be a normal vector to γ. For the points of the equidistant $\gamma^{+}(\delta)$ we have

$$\mathbf{x}^{+} = \mathbf{x} + \delta\mathbf{n}.$$

The cuspidal points at the ends of the dovetails on the equidistants $\gamma^{\pm}(\delta)$ are determined by the following procedure. Let us draw two geodesic lines orthogonal to the curve γ from two infinitely near points at γ. The point of intersection of these two geodesics gives the desired cuspidal point of the equidistant curve. Thus, for the cuspidal points we have

$$\lim_{\triangle s\to 0} (\mathbf{x}^{+}(s+\triangle s) - \mathbf{x}^{+}(s)) = 0.$$

Dividing the later equality by $\triangle s$ and passing to a limit at $\triangle s \to 0$ we obtain $\mathrm{d}\mathbf{x}^{+}/\mathrm{d}s = 0$. According to the Frenet formulae

$$\dot{\mathbf{x}}^{+} = \dot{\mathbf{x}} + \delta\dot{\mathbf{n}} = \dot{\mathbf{x}} - \delta k\dot{\mathbf{x}} = (1-\delta k)\dot{\mathbf{x}} = 0,$$

where upper dot denotes the derivative with respect to the natural parameter s, and k is a curvature of the curve γ. The latter equality holds only for $\delta = 1/k = R(\mathbf{x})$. The equidistants $\gamma^{\pm}(\delta)$ do not have cuspidal points if and only if δ is less than the distance to the nearest cuspidal point as is stated by inequality (6.1). □

Inequality (6.1) determines the boundaries of the stripe of unique and continuous determination of ω on the plane. The same assertion is also valid in the spherical case.

Theorem 4. *Let γ be a smooth curve on the sphere $|\mathbf{x}| = R$. The equidistants $\gamma^{\pm}(\delta)$ are smooth curves if and only if the following inequality holds:*

$$\tan\delta < \min_{\mathbf{x}\in\gamma} R/k_g(\mathbf{x}), \tag{6.2}$$

where k_g is a geodesic curvature of the curve γ.

Proof. Let γ be a smooth curve on S^2 defined by $\mathbf{x} = \mathbf{x}(s)$ with natural parameter s, i.e. $|\dot{\mathbf{x}}| = 1$. The unit vector $\dot{\mathbf{x}}$ is tangent to the curve γ and orthogonal to the vector $\mathbf{x}$; therefore $\dot{\mathbf{x}}$ is tangent to the sphere S^2. Together with the unit vector $\mathbf{b} = \mathbf{x} \times \dot{\mathbf{x}}$ the three vectors $\mathbf{x}$, $\dot{\mathbf{x}}$ and $\mathbf{b}$ form an orthogonal frame of reference. The equidistant curve $\gamma^+(\delta)$ is given by the parametric equation

$$\mathbf{x}^+ = \mathbf{x}\cos\delta + \mathbf{b}\sin\delta. \tag{6.3}$$

As in the planar case, singularities of the equidistant curve $\gamma^+(\delta)$ are specified by the condition $\mathrm{d}\mathbf{x}^+/\mathrm{d}s = 0$. According to (6.3) this gives

$$\dot{\mathbf{x}}^+ = \dot{\mathbf{x}}\cos\delta + \dot{\mathbf{b}}\sin\delta = \dot{\mathbf{x}}\cos\delta + (\mathbf{x}\times\ddot{\mathbf{x}})\sin\delta = 0. \tag{6.4}$$

Let us multiply equation (6.4) by $\dot{\mathbf{x}}$. Making the cyclic permutation in the mixed product we obtain

$$\dot{\mathbf{x}}\cdot(\mathbf{x}\times\ddot{\mathbf{x}}) = \ddot{\mathbf{x}}\cdot(\dot{\mathbf{x}}\times\mathbf{x}) = -\ddot{\mathbf{x}}\cdot\mathbf{b}.$$

The latter gives negative value of projection of acceleration vector $\ddot{\mathbf{x}}$ onto the tangent plane to sphere S^2. Indeed, the tangent plane is spanned by linear combinations of vectors $\dot{\mathbf{x}}$ and $\mathbf{b}$. The acceleration $\ddot{\mathbf{x}}$ is orthogonal to the velocity $\dot{\mathbf{x}}$ because s is a natural parameter. Hence, its projection onto the tangent plane is given by the dot product $\ddot{\mathbf{x}}\cdot\mathbf{b}$.

To conclude the proof we shall note that by definition [17] projection of acceleration in natural parametrization onto the tangent plane is referred to as the geodesic curvature k_g of the curve γ. From (6.4) it follows that

$$\cos\delta - k_g\sin\delta = 0. \tag{6.5}$$

Inequality (6.2) follows from (6.5) and from the obvious observation that the geodesic radius k_g of the curve γ on stretched sphere $|\mathbf{x}| = R$ acquires the multiplier $1/R$. □

Suppose that the curve γ on the sphere $|\mathbf{x}| = R$ is given by its spherical coordinates

$$\gamma : \begin{cases} \theta = \theta(s), \\ \varphi = \varphi(s). \end{cases}$$

We assume that $\dot\theta^2 + \sin^2\theta\,\dot\varphi^2 = 1$. The geodesic curvature can be computed by the following formula

$$k_g = -\frac{\ddot\theta}{R\dot\varphi\sin\theta} + \frac{\dot\varphi\cos\theta}{R}. \tag{6.6}$$

For the case when the curve γ has tangent points with a meridian (i.e. $\dot\varphi = 0$) one can use an equivalent formula

$$k_g = R^{-1}\sin\theta(-\ddot\theta\dot\varphi + \dot\theta\ddot\varphi) + R^{-1}\sin^2\theta\cos\theta\,\dot\varphi^3 + 2R^{-1}\cos\theta\,\dot\theta^2\dot\varphi.$$

Inequality (6.2) gives a restriction on the value of δ according to the chosen curve γ. This restriction guarantees that equidistants $\gamma^\pm(\delta)$ do not have singularities of the dovetail type. This implies the possibility of choosing the continuous branch of the function $\omega(\tau,\theta,\varphi)$ in the stripe between equidistants $\gamma^\pm(\delta)$.

There is another possibility for the non-uniqueness of the function ω on the sphere, namely, the overlapping of definition domains of the function ω over the pole. This situation is typical for the case of negative τ, $\pi/2 - \tau > \pi/2$. This is demonstrated in figure 7.

In figure 7 the curve $\gamma : \theta = \pi/2 + 1/4\sin 3\varphi$ and two equidistants $\gamma^\pm$ on the sphere $r = 1$ are shown. Here the minimal geodesic curvature of the curve γ is approximately $k_g \approx 2.14$, which is reached at $\varphi = \pi/6 + k\pi/3$, $k \in \mathbb{Z}$. According to formula (6.2) the maximal stripe, where the function ω is continuously determined, has width $2\delta = 0.86$ rad $= 50.06^\circ$.

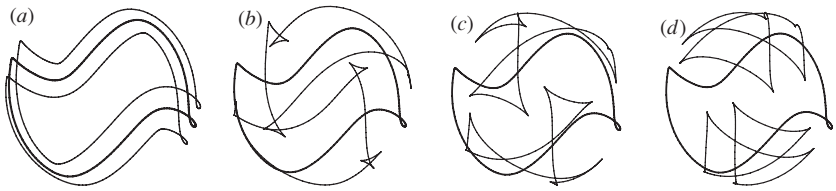

Figure 7. The overlapping of the domain of function ω over the pole. All curves lie entirely on a sphere. The middle curve is γ. Two other curves are equidistants $\gamma^{\pm}(\delta)$. The value of δ increases from figure (a) to figure (d). The domain of ω is an area on the sphere between the equidistants.

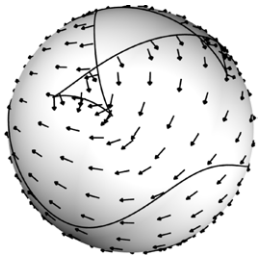

Figure 8. An example of the vector field, which satisfies equation (2.10). Curve $\gamma : \theta = \pi/2 + 1/4 \sin 3\varphi$ and its northern equidistant $\gamma^{+}(\delta)$ are shown. One can see the multiple valuedness of the vector field inside the dovetail.

The equidistants in figure 7(a) have no singularities. As δ grows the dovetails emerge at the equidistants in figures 7(b), (c). There are two branches of function ω between the equidistants inside the stripe; four branches inside the dovetails; three branches of function ω over the borders of the dovetail and one branch of ω over the equidistants $\gamma^{\pm}$ outside the dovetail. In figures 7(b) and (c) function ω is not determined in the neighbourhood of the poles. The largest value of δ is shown in figure 7(d). Here the overlapping of the areas of continuous determination of function ω over the poles takes place. In this case there are six branches of function ω near the poles of the sphere.

The vector field corresponding to the solution of equation (2.10), for the same curve γ as in figure 7, is shown in figure 8. We choose the left branch of the function ω inside the stripe between the equidistants $\gamma^{\pm}$. One can see the multiple valuedness of the vector field inside the dovetail. Further we observe the solution only inside the stripe where the function ω is uniquely determined. This stripe will be referred to as the domain stripe.

7. Construction of the solution as a whole

The results in the previous section allow us to give a description of the generalized one-dimensional plasma flow with spherical waves as a whole. The results are

- Equation (2.10) defines a curve γ on the sphere. In any section $r = \text{const}$ the solution is determined in the domain stripe of the width $\pi - 2\tau$ with the midline γ.
- For negative τ there is an overlapping of the domain stripe over the poles of the sphere. These overlapping areas should be excluded from the domain of the solution.
- The domain of the solution in the three-dimensional space is bounded by the following surfaces

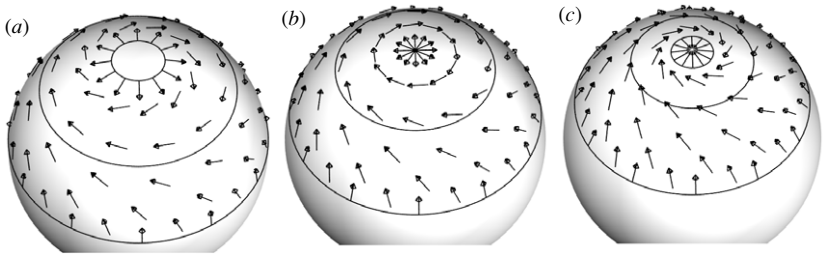

Figure 9. Examples of the initial vector field on a sphere. The middle curve γ is the parallel $\theta = \theta_* < \pi/2$. The vector field is determined in the stripe between the equidistants $\gamma^{\pm} : \theta = \theta_* \mp \delta$. Three possibilities are shown: (*a*) $\theta_* > \delta$; (*b*) $\theta_* = \delta$ and (*c*) $\theta_* < \delta$.

  - Initial spherical source or drain of plasma (if the solution cannot be prolonged up to the origin).
  - The surfaces, which are locus of the magnetic field lines originating at the boundaries of the domain stripe.

    The specified boundaries are fixed in the stationary flow and are material surfaces in the non-stationary motion.

- In the case when the function τ decreases along the magnetic field line the singularities on the boundaries of the domain stripe emerge.

For the sake of simplicity let us choose γ to be the parallel $\theta = \theta_*$ on the sphere $r = r_0$. According to formula (6.6) the geodesic curvature radius of such a curve is $R_g = 1/k_g = r_0|\tan\theta_*|$. The geodesic curvature radius is infinite whenever the parallel γ coincides with the equator $\theta = \pi/2$. This means that the conjugated points for the equator are the poles of the sphere. This is the only case when the shape of the curve γ does not imply any additional restriction on the initial data domain. The maximal domain stripe of the initial data could fulfil all the sphere surface excluding the poles. If one chose the curve γ to be parallel $\theta = \theta_* < \pi/2$ (or $\theta = \theta_* > \pi/2$) then according to formula (6.2) the domain stripe could be located only in the area between the pole $\theta = 0$ (or $\theta = \pi$) and another parallel $\theta = 2\theta_*$ (or $\theta = \pi - 2\theta_*$).

Except for the geodesic radius of the curve γ, the domain stripe of the solution is bounded by its width δ, which is defined by $\delta = \pi/2 - \tau$ where τ is taken from the solutions of the invariant subsystem (2.9). The width δ of the stripe is fixed over each sphere. As before, we assume the curve γ to be the parallel $\theta = \theta_*$. Let us observe three possibilities: (a) $\theta_* > \delta$, (b) $\theta_* = \delta$ and (c) $\theta_* < \delta$. The corresponding diagrams of the tangential component of the initial vector field are shown in figure 9. In each case the curve γ and two equidistants $\gamma^{\pm}(\delta)$ are shown. In case (a) the domain stripe of the solution does not have any singularities. The tangential direction field is regular at all points of the domain stripe. Over the equidistants $\gamma^{\pm}(\delta)$ the vector field is orthogonal to the equidistants and directed inside the stripe. In case (b) the 'northern' equidistant turns into the north pole of a sphere. At the north pole the vector field is multi-valued. Over the rest of the stripe the vector field is regular. Finally, in case (c) the domain stripe overlaps over the north pole. As before, the vector field is determined in the stripe between the equidistants with the curve γ inside. Over the equidistants the vector field is orthogonal to the equidistants. However, over the northern equidistant $\gamma^{+}(\delta)$ the vector field is directed outwards from the stripe.

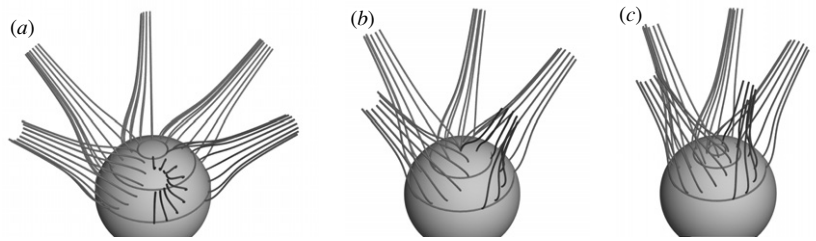

Figure 10. Typical magnetic field lines of the flow. Each magnetic line has the same shape depicted in figure 3 by the short (dashed) curve. The direction of each magnetic curve is defined by the corresponding vector field in figure 9.

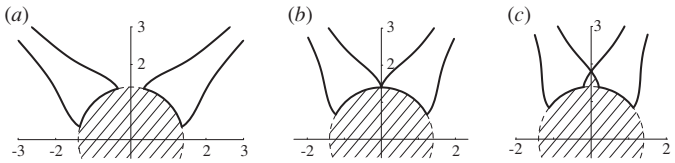

Figure 11. Axial sections of the domains of the flows in figure 10. The shaded region is the spherical source of plasma. The flow is determined only inside the area bounded by the limiting magnetic field lines (solid lines in the diagrams).

The next step of motion construction is to choose a solution for the system of equations for invariant functions (2.9). As an illustration we choose the stationary motion of incompressible plasma (3.4). Let us choose the same integral curve of equation (3.5) as we used when drawing figure 3. The initial source of plasma is the sphere $r_0 = 1.4$. Let us observe the branch of solution, which is determined by the initial data $\tau_0 = \tau(1.4) = \arccos(1/1.96)$. It corresponds to the dashed curve in figure 3.

The picture of motion generated by the described algorithm is shown in figure 10. The three diagrams in figure 10 correspond to the three possibilities for the vector field in figure 9. In figure 10(a) the solution does not have singularities. In figure 10(b) the tangential vector field is multi-valued only at the north pole of the sphere. In figure 10(c) the magnetic force lines originating at the northern equidistant intersect each other over the north pole. To avoid the collapse one could slightly narrow the domain stripe by a tiny shift of the northern boundary inside the domain stripe. The domains of the solutions in three-dimensional space are axisymmetric in all three cases. Figure 11 shows the axial section of the domains of the solution.

Figures 12 through 14 demonstrate other possible flow types. In figure 12 the curve γ is chosen to be the equator of a sphere. Pictures of the flow with the magnetic force lines defined in figure 3 are shown. In the first case, figure 12(a), the function τ is positive $0 < \tau < \pi/2$ along the magnetic line. This means that the definition stripe does not overlap over the poles of the sphere. In the second case, figure 12(b), the magnetic field lines shown by the continuous curve on figure 3 are chosen. Function τ changes from some negative value over the initial sphere $r = r_0$ to the limiting value $\tau = \pi/2$ at $r \to \infty$. For negative τ the width $\pi/2 - \tau$ of the domain stripe exceeds $\pi/2$; therefore the domain stripe overlaps over the poles. The corresponding picture of the motion is shown in figure 12(b). In order to prevent the intersection of the magnetic lines over the poles we have narrowed the domain of the initial data.

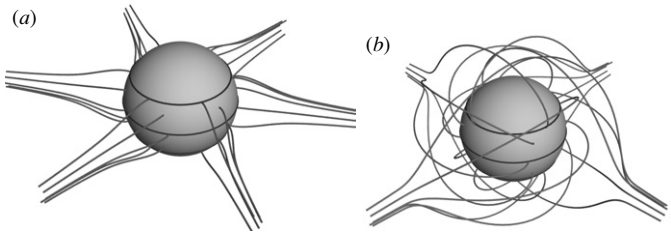

Figure 12. Examples of magnetic field lines of the flow from the spherical source. The curve γ as the equator $\theta = \pi/2$. The magnetic field line is (a) short curve; (b) long curve depicted in figure 3. The sphere is a source of plasma.

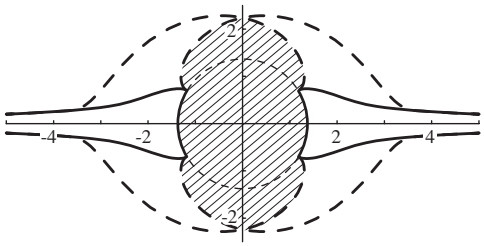

Figure 13. Axial section of the domains of the flows in figure 12. The solutions are determined outside the shaded region in the area between the limiting magnetic curves. Solid curves are boundaries of the flow depicted in figure 12(a), the dashed ones bound the flow in figure 12(b). The solid part of the boundary of the shaded region is a source of plasma.

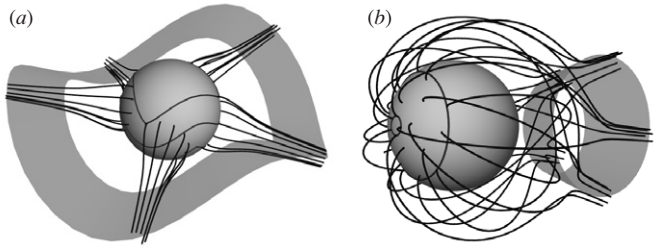

Figure 14. Examples of the plasma flow. The curve γ is (a) $\theta = \pi/2 + 1/4 \sin 3\varphi$; ($b$) $\theta = 7/8\pi$. At the infinite distance from the spherical source all particles approach the surface, which is partially shown in the diagrams.

In both cases the domain of the solution in the three-dimensional space is axisymmetric. Figure 13 shows the axial section of the domain. In both cases the solution is generated by the spherical source (it is shaded in the figure). The discharge (or drainage) of plasma takes place through the segments of the sphere shown by solid curves. The flow in figure 12(a) corresponds to the domain bounded by solid curves in figure 13. The boundaries of the flow in figure 12(b) are constructed from the dashed curves in figure 13. The boundaries of the flow are rigid conducting walls in both cases. The pressure is constant along the rigid boundaries. Therefore they could also be observed as free surfaces.

It was proved [15] that in the stationary incompressible solution under consideration function τ has a limiting value $\pi/2$ along all integral curves of equation (3.5). At the infinite

distance from the origin the flow becomes a radial one. This means that sections of the domain of the solution in three-dimensional space by spheres $r = r_0$ narrow as $r_0 \to \infty$. Thus, at infinity all plasma particles approach the surface formed by the ray, which originates at the centre of the source and slides along the curve γ. Pictures of the plasma flow, which correspond to another choice of the curve γ, are shown in figure 14. The fragments of the limiting surface are also given in these figures.

Acknowledgments

The work was partially supported by RFBR grant 05-01-00080 and by Foundation of Russian Science Support. The author expresses his gratitude to A V Penskoi for simple proof of theorem 4 and to O I Bogoyavlenskij for the invitation to Queen's University where a large part of this paper was written.

References

[1] Priest E R 1984 *Solar Magneto-hydrodynamics* (Dordrecht/Boston: Lancaster/Reidel)
[2] Baranov V V and Krasnobayev K I 1997 *Hydrodynamics Theory of The Cosmic Plasma (Gidrodinamicheskaya teoriya kosmicheskoi plazmy)* (Moscow: Nauka) (in Russian)
[3] Ovsyannikov L V 1982 *Group Analysis of Differential Equations* (New York: Academic)
[4] Ovsyannikov L V 1995 Singular vortex *J. Appl. Mech. Tech. Phys.* **36** 360–6
[5] Chupakhin A P 2003 Invariant submodels of the singular vortex *J. Appl. Math. Mech.* **67** 351–64
[6] Cherevko A A and Chupakhin A P 2004 Homogeneous singular vortex *J. Appl. Mech. Tech. Phys.* **45** 209–21
[7] Popovych H V 2000 On $SO(3)$-partially invariant solutions of the Euler equations *Proc. 3rd Int. Conf. 'Symmetry in Nonlinear Mathematical Physics'* (Kyiv: Institute of Mathematics of NAS of Ukraine) pp 180–3
[8] Grundland A M and Lalague L 1996 Invariant and partially-invariant solutions of the equations describing a non-stationary and isentropic flow for an ideal and compressible fluid in $(3+1)$ dimensions *J. Phys. A: Math. Gen.* **29** 1723–39
[9] Hematulin A and Meleshko S V 2002 Rotationally invariant and partially invariant flows of a viscous incompressible fluid and a viscous gas *Nonlinear Dyn.* **28** 105–24
[10] Fuchs J C 1991 Symmetry groups and similarity solutions of MHD equations *J. Math. Phys.* **32** 1703–8
[11] Ibragimov N H (ed) 1995 *CRC Handbook of Lie Group Analysis of Differential Equations*. (*Applications in Engineering and Physical Sciences* vol 2) (Boca Raton, FL: CRC Press)
[12] Grundland A M, Tempesta P and Winternitz P 2003 Weak transversality and partially invariant solutions *J. Math. Phys.* **44** 2704–22
[13] Anderson I M, Fels M E and Torre C G 2000 Group invariant solutions without transversality *Commun. Math. Phys.* **212** 653–86
[14] Golovin S V 2005 Singular vortex in magnetohydrodynamics *J. Phys. A: Math. Gen.* **38** 4501–16
[15] Golovin S V 2005 Invariant solutions of the singular vortex in magnetohydrodynamics *J. Phys. A: Math. Gen.* **38** 8169–84
[16] Bogoyavlenskij O I 2002 Symmetry transforms for ideal magnetohydrodynamics equilibria *Phys. Rev.* E **66** 056410
[17] Blaschke W 1930 *Differential Geometrie und Geomertische Grundlagen Einshteins Relativitätstheorie* (Berlin: Springer)